Inorg. Chem. **2007**, *46*, 9672–9677

Synthesis, Structure, and Magnetic Properties of $[(CH_3CN)_5V–O–V(CH_3CN)_5][BF_4]_4$

Julie A. Cissell,[†] Narpinder Kaur,[‡] Saritha Nellutla,[‡] Naresh S. Dalal,*[,‡] and Thomas P. Vaid*[,†]

Department of Chemistry and Center for Materials Innovation, Washington University, St. Louis, Missouri 63130, Department of Chemistry and Biochemistry and NHMFL, Florida State University, Tallahassee, Florida 32306

Received May 12, 2007

The reaction of vanadium(III) acetylacetonate with HBF_4 in acetonitrile yields $[(CH_3CN)_5V–O–V(CH_3CN)_5][BF_4]_4$, a material that serves as a convenient precursor to other $[V–O–V]^{4+}$ species such as $[(bipy)_2(CH_3CN)V–O–V(CH_3CN)(bipy)_2][BF_4]_4$ (bipy = 2,2′-bipyridine). Single-crystal X-ray diffraction shows that the V–O–V linkage of $[(CH_3CN)_5V–O–V(CH_3CN)_5]^{4+}$ is linear. An Evans method measurement of the solution-phase magnetic susceptibility indicates strong ferromagnetic coupling between the vanadium centers. Magnetic susceptibility (χ) and magnetization ($M(H)$) data for a powdered sample and for a single crystal oriented with its V–O–V axis parallel to the applied field were measured over 1.8–300 K. The results suggest that the V(III) centers are ferromagnetically coupled with $J \approx 72$ K ($\sim$50 cm^{-1}) yielding a ground state with a total spin $S_{total} = 2$. Theoretical fit to the $M(H)$ plot for the single crystal yielded $g_{||} = 2.01 \pm 0.01$ and the zero-field splitting parameter $D = 0.60 \pm 0.04$ K (0.42 ± 0.03 cm^{-1}). EPR measurements at 34 and 101.6 GHz are consistent with the $S_{total} = 2$ ground state and yield $g_{||} = 1.9825$, $g_{\perp} = 1.9725$ and $D = 0.57 \pm 0.03$ K.

Introduction

There is substantial current interest in the chemical synthesis of magnetic materials, and vanadium(III) has played a significant role in recent research on that topic. The classes of materials of interest include molecular species (single-molecule magnets), two-dimensional layered materials, and three-dimensional materials. Investigations of single-molecule magnets began with the discovery of the manganese–oxo cluster $[Mn_{12}O_{12}(O_2CCH_3)_{16}(H_2O)_4]\cdot 2CH_3CO_2H\cdot 4H_2O$[1–3] and have continued with many variations on the $Mn_{12}O_{12}$ structural motif[4] and expanded to include other metals, including vanadium(III). Although there is only one vanadium(III)-based single-molecule magnet,[5] other multinuclear vanadium–oxo clusters are known,[6,7] and V(III) has been proposed as a metal ion that would be worth exploring further for single-molecule magnets.[4] In two-dimensional materials, vanadium(III) has served as the magnetic center in layered, Kagomé-type lattices.[8–10] Finally, V(III) is a critical component of (three-dimensional) Prussian blue analogues that are magnetically ordered at room temperature[11] and even above 100 °C.[12] The relevance of V(III) to magnetic materials has prompted recent fundamental investigations of the electronic structure of the $[V(H_2O)_6]^{3+}$ ion[13] and other,

* To whom correspondence should be addressed. E-mail: vaid@wustl.edu (T.P.V.); dalal@chemmail.chem.fsu.edu (N.S.D.).
† Washington University.
‡ Florida State University.

(1) Lis, T. *Acta Crystallogr. B* **1980**, *B36*, 2042–2046.
(2) Caneschi, A.; Gatteschi, D.; Sessoli, R.; Barra, A. L.; Brunel, L. C.; Guillot, M. *J. Am. Chem. Soc.* **1991**, *113*, 5873–5874.
(3) Sessoli, R.; Tsai, H. L.; Schake, A. R.; Wang, S.; Vincent, J. B.; Folting, K.; Gatteschi, D.; Christou, G.; Hendrickson, D. N. *J. Am. Chem. Soc.* **1993**, *115*, 1804–1816.
(4) Long, J. R. In *Chemistry of Nanostructured Materials*; Yang, P., Ed.; World Scientific: Hong Kong, 2003; p 291–315.
(5) Castro, S. L.; Sun, Z.; Grant, C. M.; Bollinger, J. C.; Hendrickson, D. N.; Christou, G. *J. Am. Chem. Soc.* **1998**, *120*, 2365–2375.
(6) Laye, R. H.; Wei, Q.; Mason, P. V.; Shanmugam, M.; Teat, S. J.; Brechin, E. K.; Collison, D.; McInnes, E. J. L. *J. Am. Chem. Soc.* **2006**, *128*, 9020–9021.
(7) Mukherjee, R.; Dougan, B. A.; Fry, F. H.; Bunge, S. D.; Ziegler, C. J.; Brasch, N. E. *Inorg. Chem.* **2007**, *46*, 1575–1585.
(8) Grohol, D.; Huang, Q.; Toby, B. H.; Lynn, J. W.; Lee, Y. S.; Nocera, D. G. *Phys. Rev. B* **2003**, *68*, 094404/094401–094404/094407.
(9) Papoutsakis, D.; Grohol, D.; Nocera, D. G. *J. Am. Chem. Soc.* **2002**, *124*, 2647–2656.
(10) Grohol, D.; Papoutsakis, D.; Nocera, D. G. *Angew. Chem., Int. Ed.* **2001**, *40*, 1519–1521.
(11) Ferlay, S.; Mallah, T.; Ouahes, R.; Veillet, P.; Verdaguer, M. *Nature* **1995**, *378*, 701–703.
(12) Holmes, S. M.; Girolami, G. S. *J. Am. Chem. Soc.* **1999**, *121*, 5593–5594.
(13) Tregenna-Piggott, P. L. W.; Spichiger, D.; Carver, G.; Frey, B.; Meier, R.; Weihe, H.; Cowan, J. A.; McIntyre, G. J.; Zahn, G.; Barra, A.-L. *Inorg. Chem.* **2004**, *43*, 8049–8060.

10.1021/ic700920z CCC: $37.00
Published on Web 10/02/2007

pseudooctahedral complexes of V(III).[14] The vanadium(III) ion has a propensity to form the oxo-bridged $[V-O-V]^{4+}$ ion in aqueous solution,[15] which can be considered to be the first step toward the formation of vanadium−oxo clusters that are single-molecule magnets. The magnetic coupling between the vanadium centers of $[V-O-V]^{4+}$, where the vanadium centers are bridged only by an oxygen atom, is often ferromagnetic.[15] A large number of complexes containing a $[V-O-V]^{4+}$ core and a variety of ligands on the vanadium centers have been prepared.[16−25]

We have discovered a very simple synthesis of $[(CH_3CN)_5V-O-V(CH_3CN)_5][BF_4]_4$ by the reaction of commercially available $V(acac)_3$ (acac = acetylacetonate) and HBF_4 in acetonitrile. The $[V-O-V]^{4+}$ core is coordinated only by relatively weakly bound acetonitrile ligands, and the compound is therefore easily converted to other $[V-O-V]^{4+}$ complexes such as $[(bipy)_2(CH_3CN)V-O-V(CH_3CN)(bipy)_2]^{4+}$ by simple ligand displacement. Elaboration to larger vanadium−oxo clusters is also feasible. The V−O−V linkage in $[(CH_3CN)_5V-O-V(CH_3CN)_5]^{4+}$ is linear, and the magnetic properties of the ion will be discussed below. We note that the analogous chromium complex, $[(CH_3CN)_5CrOCr(CH_3CN)_5]^{4+}$, is known.[26]

Experimental Section

General Procedures and Materials. All manipulations were carried out using Schlenk line or glovebox techniques unless otherwise noted. Reagents were purchased from commercial suppliers and used as received unless their purification is noted as follows. Acetonitrile was distilled from P_2O_5, vacuum transferred onto 3 Å molecular sieves, and stored until it was vacuum-transferred immediately prior to use. (Acetonitrile directly from the bottle that has simply been degassed works equally as well in the synthesis and crystallization.) Infrared spectra were obtained on a Perkin-Elmer Spectrum BX FT-IR system as Nujol mulls on NaCl plates. UV−vis spectra were obtained using a Varian Cary 100 Bio UV−vis spectrometer.

Magnetic Susceptibility Measurements. Direct current magnetic susceptibility and magnetization measurements for the powder and single-crystal samples of $[(CH_3CN)_5VOV(CH_3CN)_5][BF_4]_4 \cdot 2CH_3CN$ were performed on Quantum Design SQUID magnetometer. The sample temperature was varied from 1.8 to 300 K and the field from 0 to 7 T. A single crystal was oriented in a low-susceptibility glass capillary for orientation-dependent measurements. The diamagnetic contribution from the sample holder was determined and subsequently subtracted.

EPR Measurements. Initial Q-band (ν = 34 GHz) EPR measurements were made on a Bruker Elexsys-500 spectrometer at 295 K. Additional measurements were conducted using a locally developed homodyne system at the National High Magnetic Field Laboratory, in Tallahassee, FL.[27,28]

Crystallography. Suitable crystals were obtained by slowly cooling a hot, concentrated solution of $[(CH_3CN)_5VOV(CH_3CN)_5][BF_4]_4$ in CH_3CN. All measurements were made with a Siemens SMART platform diffractometer equipped with a 1 K CCD area detector. A hemisphere of data (1271 frames at 5 cm detector distance) was collected using a narrow-frame method with scan widths of 0.30° in ω and an exposure time of 25 s/frame. The first 50 frames were remeasured at the end of data collection to monitor instrument and crystal stability, and the maximum correction on I was <1%. The data were integrated using the Siemens SAINT program, with the intensities corrected for Lorentz factor, polarization, air absorption, and absorption due to variation in the path length through the detector faceplate. A ψ scan absorption correction was applied on the basis of the entire data set. Redundant reflections were averaged. Final cell constants were refined using 7009 reflections having $I > 10\sigma(I)$, and these, along with other information pertinent to data collection and refinement, are listed in Table S1 (see Supporting Information). The Laue symmetry was determined to be 2/*m*, and from the systematic absences noted, the space group was shown unambiguously to be $P2(1)/n$. The asymmetric unit consists of one-half $[(CH_3CN)_5VOV(CH_3CN)_5]^{4+}$ on a inversion center, two BF_4^- anions, and one molecule of acetonitrile solvent of crystallization. The anions and CH_3CN solvent are all massively disordered and had to be modeled as collections of several ideal rigid bodies with varying occupancy factors.

$[(CH_3CN)_5VOV(CH_3CN)_5][BF_4]_4$. $V(acac)_3$ (10.71 g, 0.0308 mol) was dissolved in 100 mL of CH_3CN to form a yellow-brown solution. Under positive N_2 flow, an excess of HBF_4 as a solution in diethyl ether (58 mL, 54 wt %, 0.42 mol) was added via syringe, and the solution quickly turned deep red-purple. After stirring for 24 h at 22 °C, a deep purple solution and dark purple microcrystals had formed. The solution volume was reduced by half, and the product was isolated by filtration then left under vacuum for 1 h. Yield of $[(CH_3CN)_5VOV(CH_3CN)_5][BF_4]_4$: 12.48 g, 84%. The crude product can be recrystallized from acetonitrile. Anal. Calcd for $C_{20}H_{30}B_4F_{16}N_{10}OV_2$: C, 27.43; H, 3.65; N, 16.00 Found: C, 26.90; H, 3.65; N, 15.27. UV−vis (CH_3CN, nm): 239, 516, 611. IR (Nujol, cm^{-1}): 2323(s, C≡N), 2298(s, C≡N), 1287(w), 1059(s, br, BF_4), 950(m), 664(w).

$[(bipy)_2(CH_3CN)V-O-V(CH_3CN)(bipy)_2][BF_4]_4$. $[(CH_3CN)_5VOV(CH_3CN)_5][BF_4]_4$ (100 mg, 0.114 mmol) and 2,2′-bipyridine (71 mg, 0.455 mmol) were stirred in 25 mL of CH_3CN at 22 °C for 12 h. The solution was reduced to about 8 mL and benzene was added, whereupon a deep blue sticky oil formed. The volatiles were removed under vacuum, and the product was triturated with diethyl ether, yielding deep blue microcrystals. The microcrystals were filtered, and the product was held under vacuum for 1 h. Yield

(14) Krzystek, J.; Fiedler, A. T.; Sokol, J. J.; Ozarowski, A.; Zvyagin, S. A.; Brunold, T. C.; Long, J. R.; Brunel, L.-C.; Telser, J. *Inorg. Chem.* **2004**, *43*, 5645−5658.
(15) Kanamori, K. *Coord. Chem. Rev.* **2003**, *237*, 147−161.
(16) Chandrasekhar, P.; Bird, P. H. *Inorg. Chem.* **1984**, *23*, 3677−3679.
(17) Money, J. K.; Folting, K.; Huffman, J. C.; Christou, G. *Inorg. Chem.* **1987**, *26*, 944−948.
(18) Knopp, P.; Wieghardt, K.; Nuber, B.; Weiss, J.; Sheldrick, W. S. *Inorg. Chem.* **1990**, *29*, 363−371.
(19) Brand, S. G.; Edelstein, N.; Hawkins, C. J.; Shalimoff, G.; Snow, M. R.; Tiekink, E. R. T. *Inorg. Chem.* **1990**, *29*, 434−438.
(20) Zhang, Y.; Holm, R. H. *Inorg. Chem.* **1990**, *29*, 911−917.
(21) Kanamori, K.; Teraoka, M.; Maeda, H.; Okamoto, K. *Chem. Lett.* **1993**, 1731−1734.
(22) Czernuszewicz, R. S.; Yan, Q.; Bond, M. R.; Carrano, C. J. *Inorg. Chem.* **1994**, *33*, 6116−6119.
(23) Sichla, T.; Niewa, R.; Zachwieja, U.; Essmann, R.; Jacobs, H. *Z. Anorg. Allg. Chem.* **1996**, *622*, 2074−2078.
(24) Grant, C. M.; Stamper, B. J.; Knapp, M. J.; Folting, K.; Huffman, J. C.; Hendrickson, D. N.; Christou, G. *J. Chem. Soc., Dalton Trans.* **1999**, 3399−3405.
(25) Kumagai, H.; Kitagawa, S.; Maekawa, M.; Kawata, S.; Kiso, H.; Munakata, M. *J. Chem. Soc., Dalton Trans.* **2002**, 2390−2396.
(26) Andersen, N. H.; Dossing, A.; Molgaard, A. *Inorg. Chem.* **2003**, *42*, 6050−6055.
(27) Cage, B.; Hassan, A. K.; Pardi, L.; Krzystek, J.; Brunel, L.-C.; Dalal, N. S. *J. Magn. Reson.* **1997**, *124*, 495−498.
(28) Hassan, A. K.; Pardi, L. A.; Krzystek, J.; Sienkiewicz, A.; Goy, P.; Rohrer, M.; Brunel, L. C. *J. Magn. Reson.* **2000**, *142*, 300−312.

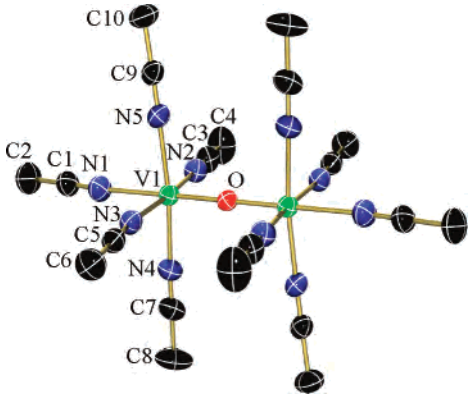

Figure 1. ORTEP view of the $[(CH_3CN)_5V-O-V(CH_3CN)_5]^{4+}$ ion in crystals of $[(CH_3CN)_5V-O-V(CH_3CN)_5][BF_4]_4 \cdot 2CH_3CN$.

Table 1. Selected Bond Distances and Angles in $[(CH_3CN)_5V-O-V(CH_3CN)_5]^{4+}$

distances (Å)		angles (deg)	
V−O	1.7549(5)	O−V−N(1)	179.70(9)
V−N(1)	2.142(3)	O−V−N(2)	92.15(8)
V−N(2)	2.088(3)	O−V−N(3)	95.29(8)
V−N(3)	2.086(3)	O−V−N(4)	93.69(8)
V−N(4)	2.083(3)	O−V−N(5)	94.41(8)
V−N(5)	2.086(3)	V−O−V	180.00(2)

of navy blue $[(CH_3CN)(bipy)_2V-O-V(bipy)_2(CH_3CN)][BF_4]_4 \cdot 2C_6H_6$: 111 mg, 73%. UV−vis ($CH_3CN$, nm): 245, 300, 519, 628. IR (Nujol, cm^{-1}): 3119 (w), 3090 (m), 3035 (w), 2321 (m, C≡N), 2284 (m, C≡N), 1602 (s), 1566 (m), 1496 (m), 1317 (s), 1283(m), 1246(m), 1164(m), 1054 (s, br, BF_4), 902 (m, br), 766 (vs), 733 (s), 687 (s), 674 (s). Anal. Calcd (Found) for $C_{56}H_{50}B_4F_{16}N_{10}OV_2$: C, 50.64 (50.91); H, 3.79 (3.71); N, 10.44 (10.55).

Results and Discussion

Synthesis. The synthesis of $[(CH_3CN)_5VOV(CH_3CN)_5][BF_4]_4$ from $V(acac)_3$ and HBF_4 in CH_3CN works equally well in either thoroughly dried CH_3CN or CH_3CN from the bottle that has been simply degassed. In the case of dry CH_3CN, the water that supplies the oxygen atom of the oxo bridge may originate from either traces of water in the HBF_4/Et_2O solution or from the aldol condensation of acetylacetone that is liberated from the $V(acac)_3$ in its reaction with HBF_4.

Synthesis of $[(bipy)_2(CH_3CN)VOV(CH_3CN)(bipy)_2][BF_4]_4$ was straightforward and achieved by the reaction of $[(CH_3CN)_5VOV(CH_3CN)_5][BF_4]_4$ with 4 equiv of 2,2′-bipyridine in CH_3CN at room temperature.

Crystal Structure. Crystals of $[(CH_3CN)_5VOV(CH_3CN)_5][BF_4]_4 \cdot 2CH_3CN$ for single-crystal X-ray diffraction were grown by slowly cooling a hot, saturated solution of $[(CH_3CN)_5VOV(CH_3CN)_5][BF_4]_4$ in CH_3CN to room temperature. A labeled ORTEP plot of $[(CH_3CN)_5VOV(CH_3CN)_5]^{4+}$ is shown in Figure 1, and a list of selected bond lengths and angles is given in Table 1. The two vanadium centers are crystallographically equivalent, and the V−O−V bond angle is a crystallographically required 180°. The coordination environment around each vanadium ion is a slightly distorted octahedron, with a small outward tilting of the CH_3CN ligands. The V−N(1) bond is longer than the other V−N bonds, presumably due to the stronger trans influence of the oxo ligand relative to the acetonitrile ligands. The V−O distance of 1.7549(5) Å is the shortest among the many V−O distances of $[V-O-V]^{4+}$ complexes that have been reported,[16−25] which range from 1.769(5) Å in $[(THF)_3Cl_2VOVCl_2(THF)_3]$[16] to 1.806(1) Å in $[(Me_3TACN)(acac)VOV(acac)(Me_3TACN)]^{2+}$ (Me_3TACN = 1,4,7-trimethyl-1,4,7-triazacyclononane).[18]

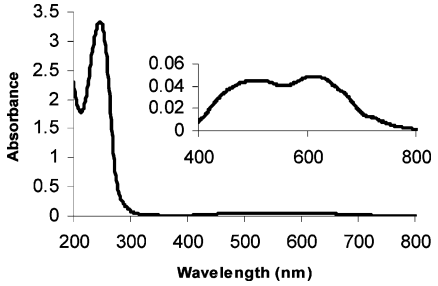

Figure 2. UV−vis spectrum of $[(CH_3CN)_5VOV(CH_3CN)_5][BF_4]_4$ in CH_3CN. Maxima are at 246, 515, and 611 nm.

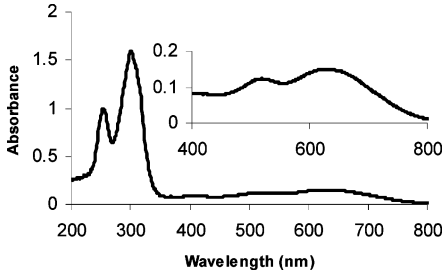

Figure 3. UV−vis spectrum of $[(bipy)_2(CH_3CN)VOV(CH_3CN)(bipy)_2][BF_4]_4$ in CH_3CN. Maxima are at 254, 300, 519, and 628 nm.

UV−Vis Spectra. The UV−vis spectrum of $[(CH_3CN)_5VOV(CH_3CN)_5]^{4+}$ in CH_3CN, shown in Figure 2, has a very intense absorption at 246 nm and two relatively weak absorptions at 515 and 611 nm. Other $[V-O-V]^{4+}$ complexes have an intense absorption that occurs between 425 and 539 nm,[18] and that absorption has been ascribed to a charge-transfer transition. In $[(CH_3CN)_5VOV(CH_3CN)_5]^{4+}$, the intensity of the absorption at 246 nm would lead us to ascribe it to a charge-transfer transition, and the two absorptions at 515 and 611 nm are simply the two expected d−d transitions of a d^2 metal center. $[V(H_2O)_6]^{3+}$, for example, has two visible absorptions at 389 and 562 nm.[29]

The UV−vis spectrum of $[(bipy)_2(CH_3CN)VOV(CH_3CN)(bipy)_2]^{4+}$, shown in Figure 3, has two intense absorptions at 254 and 300 nm. The absorption at 254 nm is presumably due to a charge-transfer transition involving vanadium and oxygen, while the new absorption at 300 nm is likely due to the $\pi-\pi^*$ transition of the coordinated bipy ligand (free 2,2′-bipy absorbs at 280 nm, and its absorption shifts upon metal coordination).[30] The two weaker absorptions at 519 and 628 nm are vanadium(III) d−d transitions.

Solution-Phase Magnetism. The magnetic coupling between the vanadium centers in previously reported

(29) Miessler, G. L.; Tarr, D. A. *Inorganic Chemistry*, 3rd ed.; Pearson Prentice Hall: Upper Saddle River, NJ, 2004.
(30) Baxter, P. N. W. *Chem. Eur. J.* **2002**, *8*, 5250−5264.

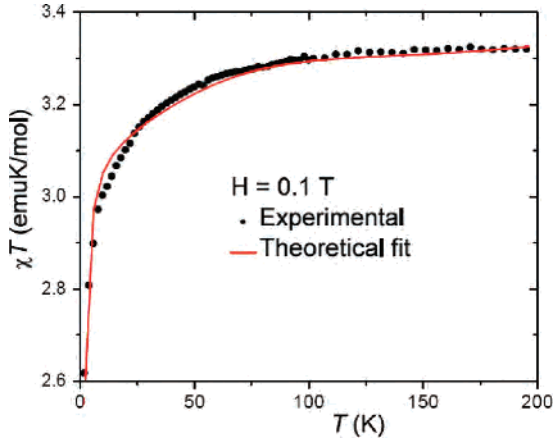

Figure 4. Temperature dependence of DC magnetic susceptibility of $[(CH_3CN)_5VOV(CH_3CN)_5][BF_4]_4$ plotted as χT. χT saturates at ~3.3 emu/K·mol. The solid line is the theoretical fit. See text for details.

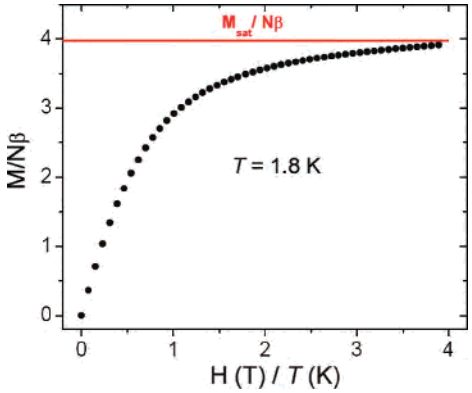

Figure 5. Reduced magnetization of a powder of $[(CH_3CN)_5VOV(CH_3CN)_5][BF_4]_4$. The saturated magnetic moment of 4 μ_B corresponds to $S_{total} = 2$.

$[V-O-V]^{4+}$ complexes ranges from weak antiferromagnetic exchange in $[(phen)_2ClV-O-VCl(phen)_2]^{2+}$ and $[(dpya)_2ClV-O-VCl(dpya)_2]^{2+}$ (phen = 1,10-phenanthroline and dpya = bis(2-pyridyl)amine)[25] to very little coupling in $[(Me_2NCH_2CH_2S)_2V-O-V(SCH_2CH_2NMe_2)_2]$[17] and $[(bipy)_2ClV-O-VCl(bipy)_2]^{2+}$[19] to strong ferromagnetic coupling in $[(Me_3TACN)(OCN)_2V-O-V(NCO)_2(Me_3TACN)]$[18] and $[LClV-O-VClL]^{2+}$ (L = 1,2-bis(2,2′-bipyridyl-6-yl)-ethane).[24] Measurements of the solution-phase magnetic susceptibility of $[(CH_3CN)_5VOV(CH_3CN)_5][BF_4]_4$ in CD_3CN by the Evans method[31,32] yielded a magnetic moment of 5.1 μ_B per $[V-O-V]^{4+}$ unit, slightly higher than the value of 4.9 μ_B expected for the $S = 2$ state that would result if the vanadium ions are ferromagnetically aligned. Clearly, there is strong ferromagnetic coupling between the vanadium centers of $[(CH_3CN)_5VOV(CH_3CN)_5]^{4+}$. Evans method measurements of the magnetic susceptibility of $[(bipy)_2(CH_3CN)VOV(CH_3CN)(bipy)_2][BF_4]_4$ in CD_3CN yielded a magnetic moment of 4.3 μ_B. If the two vanadium centers of $[(bipy)_2(CH_3CN)VOV(CH_3CN)(bipy)_2]^{4+}$ were neither ferromagnetically nor antiferromagnetically coupled, an apparent magnetic moment of 4.0 μ_B per dinuclear unit would have been observed. Thus, the measured moment of 4.3 μ_B implies a relatively weak ferromagnetic coupling in $[(bipy)_2(CH_3CN)VOV(CH_3CN)(bipy)_2]^{4+}$. The strong ferromagnetic coupling of $[(CH_3CN)_5VOV(CH_3CN)_5]^{4+}$ was further investigated by solid-state magnetic susceptibility and EPR measurements.

Solid-State Magnetic Susceptibility Measurements. In order to confirm the ferromagnetic ground state of $[(CH_3CN)_5VOV(CH_3CN)_5]^{4+}$, suggested by solution measurements, and to calculate the spin-exchange interaction J, the magnetic susceptibility (χ) measurements were performed on powder samples of $[(CH_3CN)_5VOV(CH_3CN)_5][BF_4]_4$. A plot of χT vs T is shown in Figure 4. Comparing the observed high-temperature χT value of ~3.3 emu·K/mol to the expected[33,34] value of 3 emu·K/mol for an $S_{total} = 2$ system with $g = 2.0$, it is clear that the V^{III} ions ($S_a = S_b = 1$) of the $[V-O-V]^{4+}$ unit are strongly coupled via ferromagnetic exchange interaction and that the spin ground state is $S_{total} = 2$. The mechanism underlying the magnitude of χT, ~3.3 emu·K/mol, as compared to the expected spin-only 3 emu·K/mol, is not fully understood; it can be attributed to a contribution from a small paramagnetic impurity and a term due to temperature-independent paramagnetism (TIP) (see Figure 4). Below 100 K the steady drop of χT may be attributed to the zero-field splitting of the quintet state and/or intermolecular interactions or the changing population of J spin−orbit states. However, we note that the compound is axially distorted, in which case the moment seems to become temperature independent to 'spin-only' value.[35] We thus analyzed the system using an isotropic Hamiltonian. An estimate of the spin exchange interaction J can be obtained by analyzing the susceptibility data in the following manner.

The Hamiltonian for a dinuclear entity of interacting spins S_a and S_b can be constructed as:[34]

$$\mathbf{H} = -2J\boldsymbol{S_a}\cdot\boldsymbol{S_b} + \beta H\cdot\mathbf{g_a}\cdot\boldsymbol{S_a} + \beta H\cdot\mathbf{g_b}\cdot\boldsymbol{S_b} + \boldsymbol{S_a}\cdot\mathbf{D_a}\cdot\boldsymbol{S_a} + \boldsymbol{S_b}\cdot\mathbf{D_b}\cdot\boldsymbol{S_b} \quad (1)$$

Here, the first term represents the isotropic exchange interaction, while the second and third represent the Zeeman interaction of the electrons with external field. $\boldsymbol{S_i}$ is the spin operator of the ith ion, $\mathbf{g}_i$ the g-tensor of ith ion, H the external magnetic field, and β the Bohr magneton. The last two terms represent the local or single-ion anisotropies of interacting ions S_a and S_b. On the basis of the crystal structure, we approximate axial symmetry at each V^{III} center, with V−O−V axis as the symmetry axis. The Hamiltonian in eq 1, can then be rewritten as:[34]

$$\mathbf{H} = -2J\boldsymbol{S_a}\cdot\boldsymbol{S_b} + \beta g_{au}H_u\boldsymbol{S_{au}} + \beta g_{bu}H_u\boldsymbol{S_{bu}} + D_a[\boldsymbol{S_{az}}^2 - S_a(S_a+1)/3] + D_b[\boldsymbol{S_{bz}}^2 - S_b(S_b+1)/3] \quad (2)$$

(31) Evans, D. F. *J. Chem. Soc.* **1959**, 2003−2005.
(32) Vaid, T. P.; Lytton-Jean, A. K.; Barnes, B. C. *Chem. Mater.* **2003**, *15*, 4292−4299.
(33) Carlin, R. L. *Magnetochemistry*; Springer-Verlag: New York, 1986.
(34) Kahn, O. *Molecular Magnetism*; VCH: New York, 1993.
(35) Vulfson, S. G. *Molecular Magnetochemistry*; Taylor and Francis: London, 1998.

where, index 'u' denotes the direction of the applied magnetic field, g_{iu} and $\boldsymbol{S}_{iu}$ are, respectively, the principal g value and spin operator of the ith ion along the direction 'u'. D_i is the axial zero-field splitting parameter of ith ion. If the isotropic exchange interaction $-2J\boldsymbol{S}_a\cdot\boldsymbol{S}_b$ is the leading term in eq 2, as is in our case, the total spin quantum number S_{total}, characterizing the spin of dinuclear states, is a good quantum number.[34] S_{total} varies from $|S_a - S_b|$ to $S_a + S_b$ with corresponding energies $E_{(2)} = 0$, $E_{(1)} = 4J$, and $E_{(0)} = 6J$. Furthermore, these dinuclear states are energetically well separated from each other and the zero-field splittings of the excited states do not contribute to the magnetic properties.[34]

Considering the fact that the observed χT profile is mainly representative of an $S_{total} = 2$ ground state, we formulate an effective Hamiltonian $\mathbf{H_{eff}}$, shown in eq 3.

$$\mathbf{H_{eff}} = \beta g_{2,u} H_u \boldsymbol{S}_u + D_2[\boldsymbol{S}_z^{\,2} - 2] \tag{3}$$

g_2 and D_2 are respectively related to g_a, g_b and D_a, D_b, as shown in eqs 4 and 5.[34]

$$g_{2,u} = \frac{g_{a,u}}{2} + \frac{g_{b,u}}{2} \tag{4}$$

$$D_2 = \frac{D_a}{6} + \frac{D_b}{6} \tag{5}$$

The principal magnetic susceptibilities $\chi_{||}$ and $\chi_\perp$, shown in eqs 6 and 7,[36] can then be calculated by introducing the eigenvalues corresponding to eq 3 for H || z and H || $x(y)$ along with the thermal population of the excited triplet and singlet states into the van Vleck equation.[34] Table S1 in the Supporting Information gathers the coefficients $E_n^{(0)}$, $E_n^{(1)}$, and $E_n^{(2)}$ as they appear in the van Vleck equation.

$$\chi_{||} = \left(\frac{2Ng_{||}^{\,2}\beta^2}{k_B T}\right) \left[\frac{e^{(D_2/k_BT)} + 4\,e^{(-2D_2/k_BT)} + e^{(-4J/k_BT)}}{e^{(2D_2/k_BT)} + 2\,e^{(D_2/k_BT)} + 2\,e^{(-2D_2/k_BT)} + 3\,e^{(-4J/k_BT)} + e^{(-6J/\mathbf{k}_BT)}}\right] \tag{6}$$

$$\chi_\perp = \left(\frac{2Ng_\perp^{\,2}\beta^2}{k_B T}\right) \left[\frac{(k_BT/3D_2)[9\,e^{(2D_2/k_BT)} - 7\,e^{(D_2/k_BT)} - 2\,e^{(-2D_2/k_BT)}] + e^{(-4J/k_BT)}}{e^{(2D_2/k_BT)} + 2\,e^{(D_2/k_BT)} + 2\,e^{(-2D_2/k_BT)} + 3\,e^{(-4J/k_BT)} + e^{(-6J/k_BT)}}\right] \tag{7}$$

$$\chi_{dinuclear} = (\chi_{||}/3) + (2\chi_\perp/3) \tag{8}$$

We used $g_a = g_b = g$ and $D_a = D_b = D$, which implies that $g_2 = g$ and $D_2 = D/3$ (cf. eqs 4 and 5), because the $[V-O-V]^{4+}$ unit is centrosymmetric. Furthermore, $S_a = S_b$ and $g_S = (g_a + g_b)/2$ for all values of total spin S_{total}.[34]

To reproduce the powder experimental χT profile shown in Figure 4, paramagnetic susceptibility[33,34] from a mono-

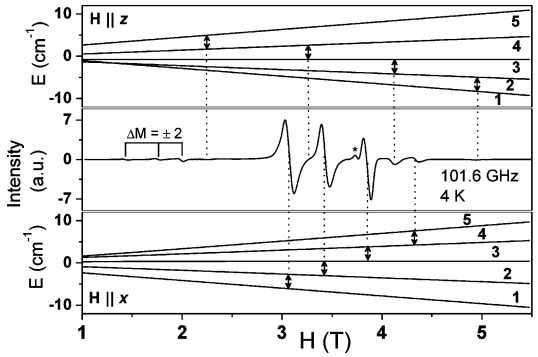

Figure 6. EPR spectrum of a powdered sample of $[(CH_3CN)_5VOV(CH_3CN)_5][BF_4]_4$ at 101.6 GHz and 4 K along with the energy level diagram for an $S = 2$ system for a field oriented parallel to the z axis (top) and x axis (bottom). The four double-headed arrows in the energy level diagram correspond to the four allowed transitions in the experimental spectrum (middle). The peak marked by '*' is ascribed to a paramagnetic impurity, likely to be a triplet state, following the magnetic susceptibility data.

nuclear $S = 1$ impurity (denoted by x) had to be taken into account along with the dinuclear susceptibility given in eq 9. An additional term due to TIP was also included as a floating parameter.

$$\chi = x\chi_{dinuclear} + (1 - x)^* \left[\frac{Ng^2\beta^2 s(s+1)}{3k(T-\theta)}\right] + \chi_{TIP} \tag{9}$$

In order to reduce the number of fitting parameters, $g_{||}$ was set equal to $g_\perp$. The theoretical fit to eqs 6−9, shown as solid red line in Figure 4, is considered satisfactory. The fitting parameters are: $g = 2.11 \pm 0.01$, $|D_2| = 2.34 \pm 0.08$ K, $J = 72 \pm 5$ K, $\theta = -10.0$ K (fixed) and $x = 0.90$ (fixed), and TIP $= 0.0013 \pm 0.0001$ emu/mol. The large uncertainties might be due to various approximations invoked in the theoretical derivations, in particular, the omission of the spin−orbit coupling effects. The overall magnitudes of g, D, and J are in agreement with other vanadium dinuclear compounds containing a $[V-O-V]^{4+}$ unit in which the vanadium ions are strongly ferromagnetically coupled.[18,24]

Magnetization Measurements and Analysis. Further affirmation of the ferromagnetic ground state of $[V-O-V]^{4+}$ unit was attained from the magnetization measurements performed on powder and single-crystal samples $[(CH_3CN)_5VOV(CH_3CN)_5][BF_4]_4$. Using the standard formula for paramagnetic saturation, $M_{sat}/N\beta = gS$, it is clear that for an $S_{total} = 2$ system, the saturation reduced magnetization, $M_{sat}/N\beta$, should approach 4.0 if $g = 2$. Indeed, the magnetization of the $[V-O-V]^{4+}$ powder sample, as shown in Figure 5, approaches the expected value of 4. Similar behavior was observed for the single-crystal sample for H || 001 axis and the data was fit to eqs S1−S3 (see Supporting Information) to parameters $|D_2| = 0.60 \pm 0.04$ K and $g_{||} = 2.01 \pm 0.01$ (see Figure S1, Supporting Information). The quality of fit is not very satisfactory. Again, this discrepancy might be pointing to the inadequacy of the isotropic Hamiltonian used herein. The need for further improvement in the theoretical analysis seems to be clear. In addition, the sample orientation was fixed only approximately (visually). Nevertheless, the data are consistent with our main conclusions from the powder measurements.

(36) O'Connor, C. J. *Prog. Inorg. Chem.* **1982**, *29*, 203−283.

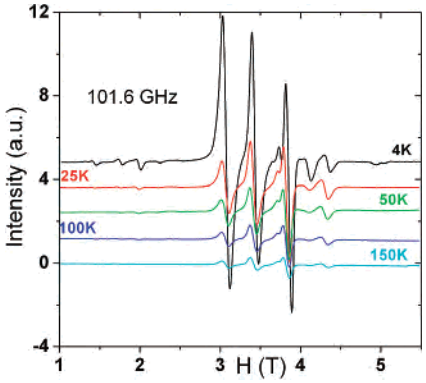

Figure 7. Temperature dependence of powder EPR spectra of $[(CH_3CN)_5VOV(CH_3CN)_5][BF_4]_4$ at 101.6 GHz. The higher intensity of the high-field perpendicular peak indicates that the zero-field splitting parameter D is positive.

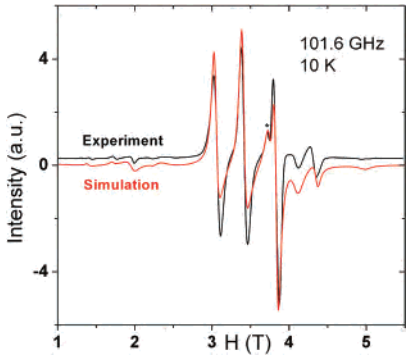

Figure 8. Experimental and simulated powder EPR spectra of $[(CH_3CN)_5VOV(CH_3CN)_5][BF_4]_4$ at 101.6 GHz and 10 K. The experimental spectrum was simulated using $S = 2$ and a Lorentzian line shape, and the parameters listed in the text. The peak marked by '*' is thought to be from an impurity triplet state. The Hamiltonian parameters for the triplet state of the impurity are $g \approx 2.0$ and $D = 0.50$ K.

Electron Paramagnetic Resonance (EPR). EPR spectroscopy probes the spin ground state directly and provides more precise Hamiltonian parameters. The middle panel of Figure 6 shows a typical EPR spectrum of powdered $[(CH_3CN)_5VOV(CH_3CN)_5][BF_4]_4$ at 101.6 GHz and 4 K. The four possible transitions of an $S_{total} = 2$ system, shown as double-headed arrows in Figure 6, match the observed peaks fairly well, validating that the ground state is quintet ($S_{total} = 2$). The peaks marked by '*' arise from a mononuclear $S = 1$ impurity, x. Temperature dependence of EPR spectra at 101.6 GHz is shown in Figure 7. As temperature increases, the intensity shifts into the high-field peak, establishing that the zero-field splitting parameter D_2 is positive.

The Spin Hamiltonian given in eq 3 was utilized in simulating the observed EPR spectra using locally developed programs.[37,38] However, the magnetic hyperfine interaction, $\boldsymbol{I}\cdot\boldsymbol{A}\cdot\boldsymbol{S}$, between the magnetic moment of the nucleus of spin I and an ion of spin S was neglected in the simulations because the hyperfine−fine structure from ^{51}V ($I = 7/2$) was not resolved in our EPR measurements, essentially because of the fast electron−electron exchange coupling between the vanadium centers. This conclusion is consistent with the fact that there seems to be only one example where ^{51}V hyperfine structure has been resolved for an integral spin system.[39] In that system, the vanadium ions were doped at a low concentration in a diamagnetic host, so spin exchange was significantly reduced. Figure 8 displays the experimental and simulated powder EPR spectra of $[(CH_3CN)_5VOV(CH_3CN)_5][BF_4]_4$ at 101.6 GHz and 10 K. The agreement between the simulated and experimental spectra is considered reasonable, even though the intensities of some of the peaks do not quite match the observed ones. The discrepancy is ascribed to linewidth effects and the powder nature of the sample. The simulated parameters for the quintet ground state are $g_\perp = 1.9725 \pm 0.0005$, $g_{||} = 1.9825 \pm 0.005$, and $D_2 = 0.57 \pm 0.03$ K. The impurity signal is consistent with a species with $S = 1$; $g \approx 2$ and $D \approx 0.5$ K.

Conclusions

A new $[V-O-V]^{4+}$ complex, $[(CH_3CN)_5VOV(CH_3CN)_5][BF_4]_4$, was synthesized by the reaction of $V(acac)_3$ and HBF_4 in CH_3CN. It was characterized by single-crystal X-ray diffraction and magnetic measurements. DC magnetic susceptibility, magnetization, and EPR measurements show that the complex has a ground state spin $S_{total} = 2$, indicating that the two V(III) centers are ferromagnetically coupled with $J \approx 50$ cm^{-1}. The low-temperature decrease in χT is ascribed to the zero-field splitting term ($D \approx 0.57 \pm 0.03$K) and an intermolecular antiferromagnetic interaction. The positive value of D implies that $[(CH_3CN)_5VOV(CH_3CN)_5]^{4+}$ cannot be a single-molecule magnet. This easily accessible compound serves as a convenient precursor to other $[V-O-V]^{4+}$ complexes and possibly larger vanadium−oxo clusters.

Acknowledgment. We thank James Korp of the University of Houston for solution of the crystal structure. The work at FSU was supported in part by NSF Grant No. NIRT-DMR 0506946. NHMFL is a national users facility funded through Cooperative Agreement Grant No. DMR-0084173 and the State of Florida.

Supporting Information Available: Crystal structure data in CIF format and crystallographic details, single-crystal magnetization, and the derivation of the equations used in the theoretical analysis. This material is available free of charge via the Internet at http://pubs.acs.org.

IC700920Z

(37) vanTol, J. *EPRCalc*; National High Magnetic Field Laboratory: Tallahassee, FL.

(38) Ozarowski, A. *Spin*; National High Magnetic Field Laboratory: Tallahassee, FL.

(39) Tregenna-Piggott, P. L. W.; Weihe, H.; Bendix, J.; Barra, A.-L.; Guedel, H.-U. *Inorg. Chem.* **1999**, *38*, 5928−5929.